Excitation Energy Trapping by the Reaction Center of *Rhodobacter Sphaeroides*

ANA DAMJANOVIĆ, THORSTEN RITZ, KLAUS SCHULTEN

Theoretical Biophysics, Beckman Institute, University of Illinois at Urbana–Champaign, Urbana, Illinois 61801

Received 21 July 1999; revised 7 September 1999; accepted 10 September 1999

ABSTRACT: The excitation energy transfer between light-harvesting complex I (LH-I) and the photosynthetic reaction center (RC) of the purple bacterium *Rhodobacter (Rb.) sphaeroides* is investigated on the basis of the atomic level structures of the two proteins, assuming a ring-shaped model for LH-I. Rates of excitation energy transfer are calculated, based on Förster theory. The LH-I and RC electronic excitations are described through effective Hamiltonians established previously, with parameters derived from quantum chemistry calculations by Cory and co-workers. We also present an effective Hamiltonian description with parameters based on spectroscopic properties. We study two extreme models of LH-I excitations: electronic excitations delocalized over the entire LH-I ring and excitations localized on single bacteriochlorophylls. The role of accessory bacteriochlorophylls in bridging the excitation energy transfer is investigated. The rates of back-transfer, i.e., RC → LH-I excitation energy transfer, are determined, too. Int J Quant Chem 77: 139–151, 2000

Key words: light-harvesting complexes; photosynthetic reaction center; excitation energy transfer; Förster theory; excitons

Correspondence to: K. Schulten.
Contract grant sponsor: National Science Foundation.
Contract grant numbers: NSF BIR 94-23827 EQ; NSF BIR 93-18159.
Contract grant sponsor: National Institutes of Health.
Contract grant number: NIH PHS 5 P41 RR05969-04.
Contract grant sponsor: Carver Charitable Trust.

 CCC 0020-7608 / 00 / 010139-13

Introduction

In photosynthesis, light energy is absorbed by specialized chromophore–protein aggregates, the so-called light-harvesting (LHs) complexes. This energy is transferred with great efficiency to the photosynthetic reaction center (RC), where it is utilized for charge separation [1–3]. The absorbed light energy is funneled into the RC in the form of electronic excitations of chromophores associated with the LHs [4, 5]. In purple bacteria, the RC is directly surrounded by the so-called light-harvesting complex I (LH-I). LH-I is in turn surrounded by several smaller light-harvesting complexes, LH-IIs, and in some purple bacteria, LH-IIIs. The LH-I → RC excitation energy transfer takes about 37 ps at temperatures between 100 and 177 K and probably also between 100 and 300 K [6, 7]. This transfer time is an order of magnitude longer than the initial electron transfer step in the reaction center, thus making the RC a sink of excitation energy. In a series of excitation energy transfer steps between LHs and the RC, LH-I → RC transfer is the rate-limiting step occurring an order of magnitude slower than transfers between different LHs, which occur on a picosecond timescale [8].

Energy transfer between LH-I and the RC involves predominantly the near-infrared, the so-called Q_y excitations of bacteriochlorophylls (BChls). BChls of the RC and of the modeled structure of LH-I are shown in Figure 1. Directions of transition dipole moments of Q_y states are also displayed in Figure 1. Due to limited knowledge of the excitonic interactions and couplings to the protein motions, as well as due to the lack of a crystal structure of LH-I, the exact nature of the electronic states participating in energy transfer is not well understood. However, the relatively large separation between LH-I and RC BChls (about 40 Å on average) indicates that the mechanism of excitation energy transfer is almost certainly the Förster mechanism [10].

An atomic level structure of LH-I of purple bacterium *Rhodobacter (Rb.) sphaeroides* had been computationally modeled [11] and was found to be in agreement with an 8.5-Å resolution electron microscopy projection map of the highly homologous LH-I of *Rhodospirillum (Rs.) rubrum* [12]. The electron microscopy map of LH-I displays a closed ring structure. The ring structure of LH-I is, however, questioned by some researchers. For example, the authors in [13] argue that such a structure might be an artifact caused by averaging of electron microscopy data and have recently proposed an open, C-shaped structure of LH-I of *Rb. sphaeroides*. A 20-Å projection map of the C-shaped LH-I was superimposed with the projection map of $\frac{3}{4}$ of LH-I of *Rs. rubrum* [12], revealing significant overlap of the two structures [13]. The structure of LH-I around the RC may also be species dependent.

In our calculations, we assume a ring-shaped LH-I, for which an atomic level model is available [11]. This model structure [11, 12] displays a hexadecamer containing 32 BChls and 16 carotenoids as protein cofactors (see Fig. 1). The close proximity of BChls in the model of LH-I (Mg–Mg separation about 9.2 Å) leads to excitonic interactions between BChl Q_y electronic excitations [14, 15]. The length of exciton delocalization depends on the strength of the coupling between the BChls as well as on the effective structural and dynamical disorder. None of the latter three has been precisely determined. For the light-harvesting complex II (LH-II), structurally similar to LH-I, estimates of the exciton delocalization length at room temperature vary from that of a complete ring [16], to only two BChls [17]. An estimate of the delocalization length in LH-I suggested in [18, 19] is 3–4 BChls.

The photosynthetic reaction center of the purple bacterium *Rb. sphaeroides* is one of the first membrane proteins for which a crystal structure has been solved [20, 21] (see Fig. 1). It contains four BChls, two bacteriopheophytins (BPhs), one carotenoid, and two ubiquinone molecules as chromophores. Two of the BChls, denoted as the special pair ($P_{A/B}$ in Fig. 1), are strongly coupled; the special pair electronic excitations form excitons, with upper and lower excitonic component commonly referred to as P_+ and P_-. P_- is the primary electron donor in a series of electron transfer steps within the RC, the first of which occurs in about 3 ps [22]. The efficiency of LH-I → RC excitation energy transfer depends on the rates of the primary electron transfer step, the LH-I → RC transfer, as well as on the RC → LH-I excitation energy back-transfer.

The role of the other two BChls in the RC, the so-called accessory BChls (B_A and B_B in Fig. 1), is still a subject of investigations [23–25]. It is widely accepted that they are involved in electron transfer [26–28]. Furthermore, it is thought that the electronic states of the accessory BChls mix with the P_+ state [29–32]. Accessory BChls could, thus, speed up the excitation energy transfer from LH-I by effectively bridging the distance between LH-I BChls and the special pair, as suggested in [14].

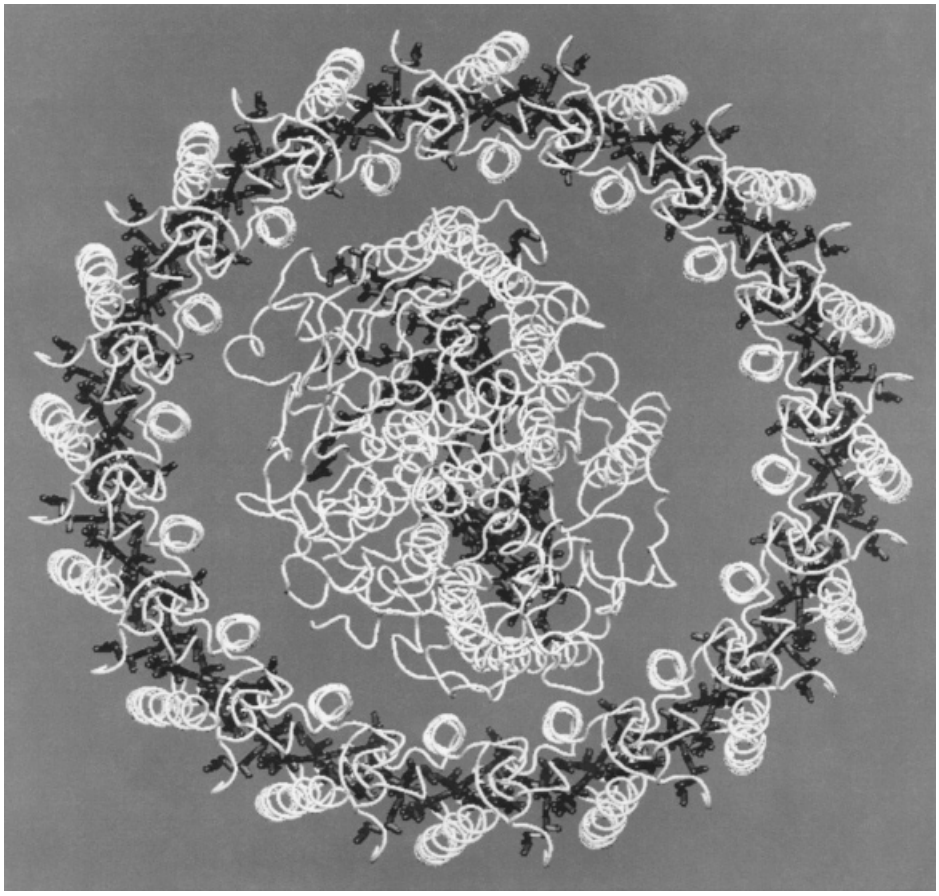

(a)

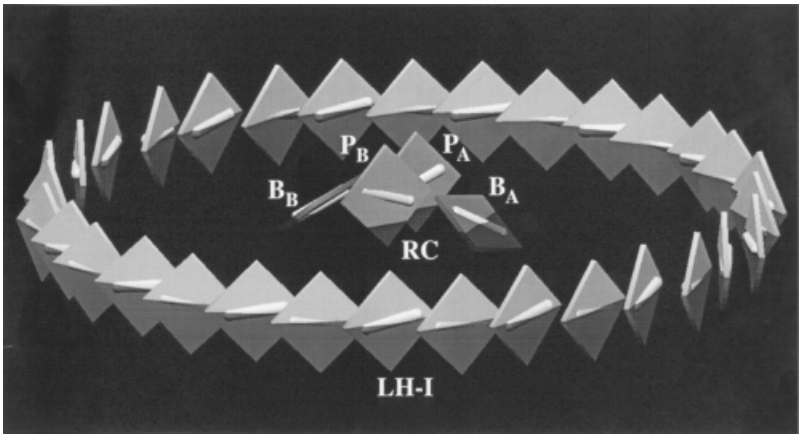

(b)

FIGURE 1. Modeled structure of the LH-I–RC complex. (a) Top view displays RC structure encompassed by the LH-I ring. Protein components of LH-I and RC are shown as white; BChls, bacteriopheophytins and carotenoids are in black. (b) Arrangements of BChls in the LH-I–RC pair, side view. The BChls are represented as squares, and the RC special pair (P_A, P_B) and accessory BChls (B_A, B_B) are labeled; the bars represent the direction of the BChl Q_y transition dipole moments (produced with the program VMD [9]).

In this study, we investigate the LH-I → RC excitation energy transfer by calculating the respective transfer rates. The calculations rely on the availability of the modeled structure of LH-I [11], as opposed to the previous descriptions of LH-I → RC excitation energy transfer [33–35], and are based on the atomic level structures of both LH-I and the RC of a single purple bacterium (*Rb. sphaeroides*). Calculations of the transfer rates are based on Förster theory. Since the exact LH-I exciton delocalization length has not been determined, the present calculations consider two extreme models of electronic excitations of LH-I, the case of Q_y excitons delocalized over the entire ring, and the case of Q_y excitations localized on single BChls. We also study two models for the RC excitations, both based on the effective Hamiltonian approach presented in [14]. In the first model the effective Hamiltonian includes the $P_{A/B}$ Q_y states only; in the second model the effective Hamiltonian includes both the $P_{A/B}$ and the $B_{A/B}$ Q_y excitations. More extensive calculations of the excited states of the RC have been presented elsewhere [29, 30, 36, 37], and our description of the RC excitons, based on the Q_y excitations only, and not including vibrational couplings and couplings to charge transfer states, is a rough but effective approximation, sufficient for an estimate of excitation energy transfer rates. The description of delocalized excitons in LH-I relies on the effective Hamiltonian introduced previously [14]. Parameters of the effective Hamiltonian were derived from computationally costly quantum chemistry calculations carried out for special chlorophyll aggregates, i.e., those studied by Cory et al. [38] and Hu et al. [14].

However, the inter-chlorophyll couplings, derived from quantum chemistry simulations [14, 38, 39], are too large compared to experimentally estimated parameters. For consistency with our previous effective Hamiltonian description in [4] and the quantum chemistry calculation in [38], we will first calculate the LH-I → RC couplings with the quantum chemistry set of parameters. The calculated couplings will next be scaled down to make up for the overestimate of the quantum chemistry parameters compared to the experimental parameters. However, we will also calculate the LH-I → RC couplings by employing purely the parameters suggested by experiments [31, 40–42]. The results obtained with the scaled down quantum chemistry parameter sets, and experimental parameter sets will be compared.

In the summary of our results we suggest the pathway for excitation energy transfer within the model of completely delocalized LH-I excitons, discuss the role of accessory BChls in LH-I → RC excitation energy transfer, as well as the ratio of rates for forward (LH-I → RC) and backward (RC → LH-I) excitation energy transfer.

Method and Notation

Rates of excitation transfer between donor and acceptor are calculated according to the formula [10]

$$k_{DA} = \frac{2\pi}{\hbar}|U_{DA}|^2 J_{DA}, \qquad J_{DA} = \int S_D(E) S_A(E)\, dE. \tag{1}$$

The rate depends on the electronic coupling between donor and acceptor states (U_{DA}) and on the spectral overlap (J_{DA}) between normalized donor emission [$S_D(E)$] and acceptor absorption spectra [$S_A(E)$]. $S_D(E)$ and $S_A(E)$ are approximated by Gaussians, with parameters $E_{D(A)}$ [emission (absorption) energy maximum], and $\Gamma_{D(A)}$ [full width at half-maximum], estimated from experiments and calculations [14, 43, 44].

The coupling between the nth excited state of the donor (LH-I) and the kth excited state of the acceptor (RC) can be approximated as follows:

$$U_{DA} = \langle \boldsymbol{\alpha}_n | \hat{W} | \boldsymbol{\beta}_k \rangle = \sum_{i=1}^{N} \sum_{j=1}^{M} \alpha_{n,i} \beta_{k,j} W_{i,j}. \tag{2}$$

Here $\boldsymbol{\alpha}_n$ and $\boldsymbol{\beta}_k$ are the eigenvectors of the nth excited state of the donor and kth excited state of the acceptor (with coefficients $\alpha_{n,i}$ and $\beta_{k,j}$), respectively. $\hat{W}$ is a matrix of induced dipole – induced dipole couplings, namely,

$$W_{i,j} = \left(\frac{\mathbf{d}_i \cdot \mathbf{d}_j}{r_{ij}^3} - \frac{3(\mathbf{r}_{ij} \cdot \mathbf{d}_i)(\mathbf{r}_{ij} \cdot \mathbf{d}_j)}{r_{ij}^5} \right), \tag{3}$$

where i, j denote the individual BChls in LH-I and the RC. Here $\mathbf{d}_i$ and $\mathbf{d}_j$, respectively, are the transition dipole moments between the ground state and the Q_y state of BChl i of LH-I and BChl j of the RC, while $\mathbf{r}_{ij}$ is a vector connecting Mg atoms of BChls i and j. The orientations of the Q_y transition dipole moments were determined from the geometries of BChls in LH-I and the RC, as defined by the vector connecting the N atom of pyrrol I and the N atom of pyrrol III; the transition dipole moments are indicated in Figure 1. The magnitudes of Q_y transition dipole moments were set to 11 D, as estimated from the effective Hamiltonian and quantum chemistry calculations [14, 38]. The value of the dielectric constant used in our calculations is $\epsilon = 1$.

In case of a localized description of LH-I excitations, the donor state involves a Q_y excitation of a single BChl (e.g., BChl k) and, hence, $\alpha_{n,i} = \delta_{i,k}$. In case of a delocalized description, the eigenvectors $\boldsymbol{\alpha}_n$ of the nth excitonic state of LH-I are determined from the effective Hamiltonian [14, 15], which describes 32 ($N = 32$) tightly coupled BChls of the LH-I ring; the interactions between nonneighboring BChls are described by Eq. (3); the couplings between nearest neighbors cannot be approximated in this fashion and are given the values 806 and 377 cm^{-1}, as suggested in [14] by fitting the effective Hamiltonian spectrum of LH-II to the spectrum obtained from the quantum chemistry calculation reported in [38].

The model for the excitonic states of the RC is described in detail in [14, 15]. As suggested in [39], the special pair coupling was assumed to be 1000 cm^{-1}, while all other couplings were calculated using Eq. (3). Two cases, an exciton localized on the special pair, $P_{A/B}$ ($M = 2$) and an exciton spreading over $P_{A/B}$ and $B_{A/B}$ ($M = 4$), were treated and, accordingly, coefficients $\beta_{k,j}$ in Eq. (2) were provided [14]. The latter coefficients determine the amount of mixing of $P_{A/B}$ and $B_{A/B}$ excitations within a particular excitonic state and imply that the lowest exciton state of the RC has 79% special pair character and 21% accessory BChl character [14]; the latter model overestimates the mixing of the accessory BChl into the lowest exciton state, which most probably has no accessory BChl character. To avoid this problem, we will present further below another set of calculations with an experimentally determined set of Hamiltonian matrix elements that furnish presumably a better description of the RC excitations.

DEFINITION OF ELECTRONIC STATES AND COUPLINGS

The LH-I excitations were described as (1) localized on single BChls and (2) delocalized over the entire ring. The LH-I BChl that is most strongly coupled to a particular exciton state of the RC is labeled $BChl^M$. In the notation employed here, $BChl^M(Q_y)$ describes the Q_y excitation of $BChl^M$ and n_k(LH-I) denotes the kth excitonic state of LH-I delocalized over the entire ring. Numbering of different BChls is shown in Figure 2. The two models of RC excitons assume (1) delocalization over the special pair $P_{A/B}$ only [with exciton states denoted as n_1(P) and n_2(P), corresponding to P_- and P_+] and (2) delocalization over the special pair $P_{A/B}$ and the accessory BChls $B_{A/B}$ [with exciton states denoted as n_1(P+B), n_3(P+B), n_3(P+B), and n_4(P+B)].

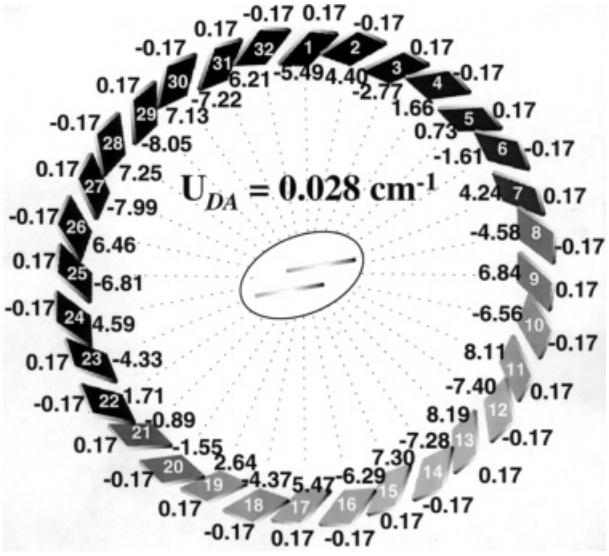

FIGURE 2. Couplings U_{DA}^{qc} between n_1(P) and (a) n_1(LH-I) as well as (b) n_2(LH-I). Couplings between individual BChl Q_y states and n_1(P) are shown within LH-I rings, in units of cm^{-1}. Numbers outside the ring denote coefficients of first and second exciton states of LH-I, i.e., $\alpha_{1,i}$ and $\alpha_{2,i}$, respectively. The numbering of individual BChls is also shown.

The couplings obtained employing the quantum chemistry set of parameters, introduced above, will be labeled as U_{DA}^{qc}. These couplings will later on be scaled down by an appropriate factor, the scaled couplings being labeled as U_{DA}^{sc}. The cou-

plings determined through effective Hamiltonian calculations employing the parameters as suggested by experiments [31, 40–42] will be labeled U_{DA}^{exp}.

Results and Discussion

We have determined couplings U_{DA} [Eq. (2)] between BChl electronic excitations of LH-I and the RC employing the two models of LH-I excitations and of the RC excitons introduced above.

COUPLINGS BASED ON QUANTUM CHEMISTRY CALCULATIONS

Figure 2 presents couplings U_{DA}^{qc} between the two lowest exciton states of LH-I, n_1(LH-I) and n_2(LH-I), and the lowest exciton state of the special pair n_1(P). Numbers inside the LH-I ring represent couplings ($U_{i,1}$) from individual BChl i to n_1(P), where $U_{i,1} = \sum_{j=1}^{M} \beta_{1,j} W_{i,j}$. Numbers outside the ring are coefficients $\alpha_{1,i}$ and $\alpha_{2,i}$ of exciton states n_1(LH-I) and n_2(LH-I). Total couplings from n_k(LH-I) to n_1(P) can be obtained as $\sum_{i=1}^{N} \alpha_{k,i} U_{i,1}$, and for n_1(LH-I) to n_1(P) is 0.028 cm^{-1} [Fig. 2(a)]. The coupling to the degenerate exciton states n_2(LH-I) and n_3(LH-I) is 27.51 and 16.64 cm^{-1}, respectively. Couplings to the energetically degenerate states should be calculated as involving that linear combination of couplings to individual states [i.e., of n_2(LH-I) and of n_3(LH-I)], that results in the largest coupling. The respective coupling is 32.15 cm^{-1} (Table I). The large difference between the coupling strength of n_1(LH-I) and $n_{2,3}$(LH-I) results from the different symmetry of these states. Due to the circular symmetry of the LH-I ring and the approximate coplanar arrangement of the Q_y transition dipole moments, the exciton state n_1(LH-I) carries nearly vanishing oscillator strength, while the states n_2(LH-I) and n_3(LH-I) together carry almost all the oscillator strength [14]. Since the RC BChls, located in the center of the LH-I ring, do not significantly disrupt the circular symmetry, the results for the coupling strengths are not surprising.

CORRECTED COUPLINGS

The magnitude of the transition dipole moments used in our calculations has been determined in [14] by fitting the effective Hamiltonian spectrum to the spectrum reported in [38]. The quantum chemistry calculation in [38] involved a single excitation configuration interaction (CI) description, which is known to overestimate transition dipole moments. Indeed, the fitting procedure mentioned above predicts the transition dipole magnitudes to be 11 D, which is larger than experimentally determined values of transition dipole moments of BChls, that range from 6.1 D [45] in organic solvent to 7.7 D [46] in BChl *a* protein from *Prosthecochloris aestuarii*. We will correct for this overestimate by scaling down the couplings U_{DA}^{qc} [Eq. (2)] by a factor $(11\ \mathrm{D}/6.3\ \mathrm{D})^2$, where 6.3 D is the magnitude of transition dipole moment employed in [47] to describe monomer Q_y transition dipoles in LH-I. The scaled-down couplings U_{DA}^{sc} are presented in Tables I and II, next to the original couplings U_{DA}^{qc}.

SPECTRAL OVERLAP

The spectral overlap integrals J_{DA} for forward as well as back-transfer were calculated according to Eq. (1). All spectral overlap integrals, together with the parameters for donor emission and acceptor absorption spectra are given in Table III.

EVALUATION OF TRANSFER RATES ACCOUNTING FOR THERMAL POPULATIONS

To determine the overall transfer rates, it is necessary to consider the Boltzmann population of exciton states. In doing so we assume that the population of exciton states equilibrates within the picosecond timescale of excitation transfer processes. Our effective Hamiltonian predicts a room temperature population of 33.3% for n_1(LH-I), 42.3% for $n_{2,3}$(LH-I), 16.4% for $n_{4,5}$(LH-I), and 8% for all other energy levels; the predicted energy gap between the n_1(LH-I) and $n_{2,3}$(LH-I) levels is 95 cm^{-1}. Recently, this gap was reported as 140 cm^{-1} at 4.2 K [49]. At room temperature the gap is expected to be smaller, about 110 cm^{-1}, close to our effective Hamiltonian prediction.

RATES FOR DELOCALIZED EXCITONS

Rates of excitation transfer were calculated according to Eq. (1), employing the scaled-down couplings U_{DA}^{sc}. The couplings, spectral overlaps, and rates of excitation energy transfer between different exciton states of LH-I and of the RC are provided in Tables I and II.

The results indicate strong coupling of the $n_{2,3}$(LH-I) states to n_1(P) [n_1(P+B)], namely $U_{DA}^{\mathrm{sc}} = 10.54\ \mathrm{cm}^{-1}$ [$U_{DA}^{\mathrm{sc}} = 14.33\ \mathrm{cm}^{-1}$]. This is not surprising since the $n_{2,3}$(LH-I) states carry almost all the oscillator strength. Observing that couplings from

TABLE I

LH-I → RC transfer rates.[a]

RC state	J_{DA} (eV^{-1})	U_{DA}^{qc} [cm^{-1} (eV)]	U_{DA}^{sc} [cm^{-1} (eV)]	k_{DA}^{sc} (1/s)
		n_1(LH-I)		
n_1(P)	6.52	0.028 (3.5×10^{-6})	0.009 (1.1×10^{-6})	8.1×10^{4}
n_2(P)	0.09	0.683 (8.5×10^{-5})	0.224 (2.8×10^{-5})	6.7×10^{5}
		$n_{2,3}$(LH-I)		
n_1(P)	7.26	32.15 (4.0×10^{-3})	10.54 (1.3×10^{-3})	1.12×10^{11}
n_2(P)	0.18	0.21 (2.6×10^{-5})	0.07 (8.5×10^{-6})	1.3×10^{5}
		$n_{4,5}$(LH-I)		
n_1(P)	7.64	0.28 (3.5×10^{-5})	0.09 (1.1×10^{-5})	9.4×10^{6}
n_2(P)	0.64	7.37 (9.1×10^{-4})	2.42 (3.0×10^{-4})	5.4×10^{8}
		BChl^{M}(Q_y)		
n_1(P)	7.26	8.19 (1.0×10^{-3})	2.69 (3.3×10^{-4})	7.6×10^{9}
n_2(P)	0.18	2.39 (9.1×10^{-4})	0.88 (3.0×10^{-4})	1.6×10^{7}

[a] RC excitons are described as a linear combination of Q_y states of $P_{A/B}$. BChl^{M} is the BChl whose Q_y excitation is most strongly coupled to the corresponding RC excitation. $M = 13$ for coupling to the n_1(P) state and $M = 9$ for the coupling to the n_2(P) state.

TABLE II

LH-I → RC transfer rates.[a]

RC state	J_{DA} (eV^{-1})	U_{DA}^{qc} [cm^{-1} (eV)]	U_{DA}^{sc} [cm^{-1} (eV)]	k_{DA}^{sc} (1/s)
		n_1(LH-I)		
n_1(P+B)	6.52	0.256 (3.1×10^{-5})	0.084 (1.0×10^{-5})	6.3×10^{6}
n_2(P+B)	0.09	3.863 (4.8×10^{-4})	1.267 (1.6×10^{-4})	2.2×10^{7}
n_3(P+B)	0.01	0.588 (7.3×10^{-5})	0.193 (7.8×10^{-6})	5.8×10^{4}
n_4(P+B)	0.02	1.869 (2.3×10^{-4})	1.869 (2.3×10^{-4})	1.0×10^{7}
		$n_{2,3}$(LH-I)		
n_1(P+B)	7.26	43.71 (5.4×10^{-3})	14.33 (1.8×10^{-3})	2.19×10^{11}
n_2(P+B)	0.18	1.68 (2.1×10^{-4})	0.55 (6.8×10^{-5})	8.0×10^{6}
n_3(P+B)	0.03	15.29 (1.9×10^{-3})	5.02 (6.2×10^{-4})	1.1×10^{8}
n_4(P+B)	0.05	0.28 (3.5×10^{-5})	0.09 (1.1×10^{-5})	6.2×10^{4}
		LH-I state: $n_{4,5}$(LH-I)		
n_1(P+B)	7.64	1.03 (1.3×10^{-4})	0.33 (4.2×10^{-5})	1.3×10^{8}
n_2(P+B)	0.64	18.85 (2.3×10^{-3})	6.18 (7.7×10^{-4})	3.6×10^{9}
n_3(P+B)	0.27	1.99 (2.5×10^{-4})	0.65 (8.1×10^{-5})	1.7×10^{7}
n_4(P+B)	0.22	9.75 (1.2×10^{-3})	3.20 (4.0×10^{-4})	3.3×10^{8}
		BChl^{M}(Q_y)		
n_1(P+B)	7.26	12.33 (1.5×10^{-3})	4.04 (5.0×10^{-4})	1.7×10^{10}
n_2(P+B)	0.18	6.16 (7.6×10^{-4})	2.02 (2.5×10^{-4})	1.1×10^{8}
n_3(P+B)	0.03	6.38 (1.0×10^{-3})	2.10 (2.6×10^{-4})	1.9×10^{7}
n_4(P+B)	0.05	3.24 (9.1×10^{-4})	1.06 (1.3×10^{-4})	8.3×10^{6}

[a] RC excitons are described as a linear combination of Q_y excitations of $P_{A/B}$ and $B_{A/B}$, using the quantum chemistry parameter set. U_{DA}^{sc} was obtained by scaling down U_{DA}^{qc} by a factor of $(11/6.3)^2$. BChl^{M} is the BChl whose Q_y excitation is most strongly coupled to the corresponding RC excitation. $M = 13, 12, 13, 11$ for couplings to the n_1(P+B), n_2(P+B), n_3(P+B), n_4(P+B) states respectively.

TABLE III

Parameters for donor emission and acceptor absorption spectra, $E_{D(A)}$ and $\Gamma_{D(A)}$, as well as spectral overlap integrals, calculated according to Eq. (1).[a]

Acceptor state	Donor state $E_{D(A)}$ ($\Gamma_{D(A)}$) (in cm^{-1})	n_1(LH-I)[b] 11,315 (575)[b]	$n_{2,3}$(LH-I)[b] 11,410 (575)[b]	$n_{4,5}$(LH-I)[b] 11,626 (575)[b]	n_1(P)[c] 10,953 (896)[c]
n_1(P)[d]	11,560 (800)[d]	6.52	7.26	7.64	
n_2(P)[d]	12,560 (800)[d]	0.09	0.18	0.64	
n_1(P+B)[d]	11,560 (800)[d]	6.52	7.26	7.64	
n_2(P+B)[d]	12,560 (800)[d]	0.09	0.18	0.64	
n_3(P+B)[d]	12,469 (460)[d]	0.01	0.03	0.27	
n_4(P+B)[d]	12,743 (800)[d]	0.02	0.05	0.22	
n_1(LH-I)[e]	11,335 (500)[e]				5.06
$n_{2,3}$(LH-I)[e]	11,430 (500)[e]				4.08
$n_{4,5}$(LH-I)[e]	11,656 (500)[e]				2.02

[a] All spectral overlaps are expressed in units of eV^{-1}.
[b] LH-I emission: absorption energies of LH-I exciton states have been calculated in [14]. To obtain the fluorescence spectrum; a Stokes shift of 20 cm^{-1} [23] was assumed. Γ_D was taken from [44].
[c] The special pair fluorescence: $E_{D(A)}$ and $\Gamma_{D(A)}$ were taken from [48]. Special pair fluorescence spectrum is needed for calculation of spectral overlap integrals for excitation energy back-transfer.
[d] Reaction center absorption: E_A and Γ_A for the special pair and accessory BChls [corresponding to n_1(P+B) and n_3(P+B)] were taken from [43]. E_A for n_2(P+B) was set to 12,560 cm^{-1}, which is the location of the upper exciton level of the special pair [n_2(P)]. However, this state is likely a mixture of P_+ and accessory BChl excitations. The location of n_4(P+B) was determined in this study (see Discussion section), with effective Hamiltonian calculations employing experimental parameters. For n_2(P+B) and n_4(P+B) Γ_A is not known, and we employ a value of 800 cm^{-1} as determined for n_1(P+B).
[e] LH-I absorption: absorption energies of LH-I exciton states have been calculated in [14].

other LH-I exciton states are weaker, and taking into account the spectral overlap integrals and Boltzmann populations, it can be concluded that in the model of completely delocalized LH-I excitons, the excitation transfer takes place from the $n_{2,3}$(LH-I) level to the n_1(P) [or to the n_1(P+B)] state.

The Boltzmann population of $n_{2,3}$(LH-I) of 42.3% results in excitation transfer times of 20.0 ps for the first model of RC excitons [$n_{2,3}$(LH-I) $\rightarrow$ n_1(P)] and 10.8 ps for the second model [$n_{2,3}$(LH-I) $\rightarrow$ n_1(P+B)] (see Tables I and II). These times are shorter than the experimentally measured time of 37 ps [7].

RATES FOR INDIVIDUALLY EXCITED BACTERIOCHLOROPHYLLS

We now calculate transfer times for individually excited BChls. Figure 2 shows that the coupling between the Q_y state of the most strongly coupled BChl, BChl^{13}, and n_1(P) is $U_{DA}^{qc} = 8.19$ cm^{-1} ($U_{DA}^{sc} = 2.69$ cm^{-1}). The coupling between BChl^{13}(Q_y) and n_1(P+B) is $U_{DA}^{qc} = 12.33$ cm^{-1} ($U_{DA}^{sc} = 4.04$ cm^{-1}). Together with a spectral overlap of 7.26 eV^{-1} the scaled-down couplings result in transfer times of 130.1 ps for the first model of RC excitons [BChl^{13}(Q_y) $\rightarrow$ n_1(P)] and 56.8 ps for the second model [BChl^{13}(Q_y)$\rightarrow$ n_1(P+B)] (see Tables I and II).

The couplings between individual BChl Q_y states n_1(P+B) are smaller than the couplings between $n_{2,3}$(LH-I) and n_1(P+B). This is to be expected, since the oscillator strength of the $n_{2,3}$(LH-I) state is enhanced relative to the oscillator strength of individual BChls Q_y states. The enhancement, due to coherency of excitations, of oscillator strength of emitting states of a group of chromophores relative to the oscillator strength of individual chromophore states is referred to as superradiance.

HAMILTONIAN WITH EXPERIMENTAL PARAMETERS: COUPLINGS AND TRANSFER RATES

We consider now predictions from an effective Hamiltonian with parameters determined from experiments. The couplings between neighboring BChls in LH-I have been assigned the values 300 and 233 cm^{-1} in [41]. The magnitude of the transition dipole moments used to calculate dipole–dipole couplings was set to 6.3 D [47]. The value of 12,121 cm^{-1} for the BChl site energy was chosen

in order to place $E_{2,3}$(LH-I) at the observed value of 875 nm (11,428 cm^{-1}).

Similarly, we set the magnitude of transition dipole moments of RC BChls to 6.3 D. The special pair coupling was estimated as 650 cm^{-1} [42] at 4.2 K, while the coupling at room temperature is expected to be about 500 cm^{-1} [31]. We employed the latter value for the special pair coupling. The site energies were varied in order to place the exciton state at 11,560, 11,469, and 12,560 cm^{-1} as suggested for the P_-, $B_{A/B}$, and P_+ states, respectively [31, 43]. A least-square fit resulted in site energy parameters $\epsilon(P_A) = \epsilon(P_B) = 12{,}092$ cm^{-1}, $\epsilon(B_B) = 12{,}568$ cm^{-1}, $\epsilon(B_A) = 12{,}594$ cm^{-1}, yielding the exciton energies E_1(P+B) = 11,577 cm^{-1}, E_2(P+B) = 12,449 cm^{-1}, E_3(P+B) = 12,576 cm^{-1}, and E_4(P+B) = 12,743 cm^{-1}. The corresponding eigenvectors in the basis (P_A, P_B, B_B, B_A) are

$$n_1 = \begin{pmatrix} 0.70 \\ -0.70 \\ 0.09 \\ -0.08 \end{pmatrix}, \quad n_2 = \begin{pmatrix} 0.50 \\ 0.51 \\ 0.51 \\ 0.47 \end{pmatrix}, \quad n_3 = \begin{pmatrix} -0.14 \\ 0.03 \\ 0.73 \\ -0.67 \end{pmatrix}, \quad n_4 = \begin{pmatrix} -0.48 \\ -0.50 \\ 0.44 \\ 0.57 \end{pmatrix}. \tag{4}$$

The lowest state n_1(P+B) has 99% special pair character and is assigned to P_-. The state n_2(P+B) is roughly a $P_+ + B_+$ combination. The state n_3(P+B) has 99% accessory BChl character and is of B_- symmetry, while the state n_4(P+B) is roughly a $P_+ - B_+$ combination. The predicted amount of mixing of the special pair and accessory BChl excitations within particular exciton states is in accordance with the current knowledge about the nature of these states [29, 31, 32].

The various couplings and transfer rates obtained with the experimental set of parameters are shown in Table IV. The corresponding transfer times are 15.8 ps [$n_{2,3}$(LH-I) $\rightarrow$ n_1(P+B)], and 102.0 ps [$BChl^{29}(Q_y) \rightarrow n_1$(P+B)] (Table IV).

COMPARISON OF COUPLINGS AND TRANSFER TIMES OBTAINED WITH TWO SETS OF PARAMETERS

The transfer times for the [$n_{2,3}$(LH-I) $\rightarrow$ n_1(P+B)] pathway, calculated with U_{DA}^{sc} and U_{DA}^{exp} are 10.8 and 15.8 ps, respectively. Similarly, the transfer times via individual BChls are 56.8 ps [$BChl^{13}(Q_y) \rightarrow n_1$(P+B), scaled quantum chemistry couplings] and 102.0 ps [$BChl^{29}(Q_y) \rightarrow n_1$(P+B), experimental couplings].

To analyze the difference in the couplings obtained with the scaled quantum chemistry and experimental sets of parameters, we recall the definition of the coupling U_{DA} [Eq. (2)]. The coupling depends on $\boldsymbol{\alpha}_n$ and $\boldsymbol{\beta}_k$, i.e., the eigenvectors of LH-I and RC excited states, and on $\hat{W}$, the matrix of induced dipole–induced dipole couplings [Eq. (3)].

Scaling down U_{DA} is equivalent to scaling down $\hat{W}$. Since the magnitude of the scaled-down quantum chemistry transition dipole moments is the same as the experimental one, i.e., 6.3 D, the matrix of induced dipole–induced dipole couplings is identical for the two sets of parameters. The difference between U_{DA}^{sc} and U_{DA}^{exp} arises, thus, from the difference in eigenvectors employed. Our calculations show that eigenvectors of LH-I excitations are almost identical for the two sets of parameters, and therefore, have negligible influence on the couplings.

Therefore, the difference between U_{DA}^{sc} and U_{DA}^{exp} is mainly due to the different description of the RC states. The quantum chemistry set of parameters predicts that the n_1(P+B) (P_-) state has 79% of special pair character and 21% of accessory BChl character [14]. Furthermore, the n_2(P+B) and n_3(P+B) states are predicted to have about 96 and 89% of accessory BChl character, respectively, and the n_4(P+B) state to have about 96% of the special pair character. This is not in agreement with the current knowledge about the nature of these states, e.g., the important P_- state is believed not to mix in any accessory BChl excitations. On the other hand, the eigenstates obtained with the experimental set of parameters predict well the amount of mixing of the special pair and accessory BChls for all of the RC states, as discussed above. The experimental set of parameters provides, therefore, more accurate results.

However, both parameter sets give the same qualitative results; the pathway of excitation transfer within the model of delocalized LH-I excitons involves the $n_{2,3}$(LH-I) state. Also, coupling via this state is stronger than the coupling via individual BChls, by approximately the same factor in both descriptions (see Tables II and IV).

ROLE OF ACCESSORY BACTERIOCHLOROPHYLLS

The role of accessory BChls in excitation energy transfer from LH-I can easily be inferred from

TABLE IV
LH-I → RC transfer rates.[a]

RC state	J_{DA} (eV^{-1})	U_{DA}^{exp} [cm^{-1} (eV)]	k_{DA}^{exp} (1/s)
		n_1(LH-I)	
n_1(P+B)	6.52	0.03 (3.7×10^{-6})	8.6×10^5
n_2(P+B)	0.09	0.81 (1.0×10^{-4})	8.6×10^6
n_3(P+B)	0.01	0.24 (3.0×10^{-5})	8.4×10^5
n_4(P+B)	0.02	1.14 (1.4×10^{-4})	3.8×10^6
		$n_{2,3}$(LH-I)	
n_1(P+B)	7.26	11.78 (1.5×10^{-3})	1.5×10^{11}
n_2(P+B)	0.18	0.61 (7.5×10^{-5})	9.8×10^6
n_3(P+B)	0.03	4.69 (5.8×10^{-4})	9.7×10^7
n_4(P+B)	0.05	0.65 (8.1×10^{-5})	3.1×10^6
		$n_{4,5}$(LH-I)	
n_1(P+B)	7.64	0.16 (2.0×10^{-5})	3.0×10^7
n_2(P+B)	0.64	4.64 (5.8×10^{-4})	2.0×10^9
n_3(P+B)	0.27	0.92 (1.1×10^{-4})	3.4×10^7
n_4(P+B)	0.22	5.17 (6.4×10^{-4})	8.6×10^8
		BChl^M(Q_y)	
n_1(P+B)	7.26	3.03 (3.8×10^{-4})	9.8×10^9
n_2(P+B)	0.18	1.56 (1.9×10^{-4})	6.4×10^7
n_3(P+B)	0.03	3.38 (4.2×10^{-4})	5.0×10^7
n_4(P+B)	0.05	1.76 (2.2×10^{-4})	2.3×10^7

[a] RC excitons are described as a linear combination of Q_y excitations of $P_{A/B}$ and $B_{A/B}$. U_{DA}^{exp} and k_{DA}^{exp} were obtained with the experimental parameter set. BChl^M is the BChl whose Q_y excitation is most strongly coupled to the corresponding RC excitation. $M = 29, 14, 13, 29$ for couplings to the n_1(P+B), n_2(P+B), n_3(P+B), n_4(P+B) states respectively.

Table IV. The calculations involving experimental parameters (Table IV) show that, in case of a completely delocalized description of LH-I excitons, the transfer occurs to the lowest state of the RC, i.e., the n_1(P+B) state. In case of a localized description the transfer also occurs into the n_1(P+B) state, due to a small spectral overlap with higher exciton states of the RC. Since the n_1(P+B) state is mainly composed of the special pair excitations, we conclude that accessory BChls play no role in excitation energy transfer.

A similar conclusion can be reached by analyzing results obtained with the quantum chemistry set of parameters. In our previous publication [14], we wrongly concluded that accessory BChls play an important role in accelerating LH-I → RC excitation energy transfer; we calculated the rate for LH-I → RC transfer assuming resonance energy transfer only between the lowest exciton state of LH-I [n_1(LH-I)] and the lowest exciton state of the RC [n_1(P) or n_1(P+B)] neglecting, thus, the important $n_{2,3}$(LH-I) → n_1(P) or $n_{2,3}$(LH-I) → n_1(P+B) pathway. The results suggested that accessory BChls play a significant role in accelerating excitation energy transfer, only because the couplings (U_{DA}^{qc}) between n_1(LH-I) − n_1(P) and n_1(LH-I) − n_1(P+B) states differ by an order of magnitude (0.028 and 0.256 cm^{-1}, Tables I and II). Our present description, which considers the excitation energy transfer from all thermally populated exciton levels using the Förster theory, does not indicate such drastic difference in couplings. For the dominant route of transfer for the two RC models, $n_{2,3}$(LH-I) → n_1(P) and $n_{2,3}$(LH-I) → n_1(P+B), the difference in couplings (U_{DA}^{qc}) is relatively small (32.15 versus 43.71 cm^{-1}, Tables I and II). The accessory BChls perturb the circular symmetry of the LH-I ring, and thus, enhance the couplings of RC exciton states with the symmetry-forbidden n_1(LH-I) state. However, since even the enhanced coupling to the symmetry-forbidden n_1(LH-I) state is much weaker than that with the strongly allowed $n_{2,3}$(LH-I) states,

the accessory BChls do not play a significant role in accelerating LH-I → RC energy transfer.

BACK-TRANSFER RATES

Let us finally consider the possibility of back-transfer, RC → LH-I. The transfer has to occur from the almost 100% populated lowest exciton state of the RC, i.e., from n_1(P) or n_1(P+B), to the exciton state $n_{2,3}$(LH-I) (other exciton states have weaker couplings, cf. Tables I, II and IV). In calculating transfer times we assumed delocalization over the complete LH-I ring. Recent single-molecule experiments on LH-II indicate that at 1.2 K the excitation is to a large extent delocalized [50] over the ring. However, there are indications that in LH-I, static inhomogeneity becomes more significant at room temperature [51], and might, thus, lead to delocalization of excitons on a fewer number of BChls.

The back-transfer times can be inferred from Tables III and IV. Of all the excitonic states of LH-I, the $n_{2,3}$(LH-I) state is most strongly coupled to the lowest exciton state of the RC and is therefore a gateway for excitation energy back-transfer. The n_1(P) → $n_{2,3}$(LH-I) [or n_1(P+B) → $n_{2,3}$(LH-I)] (scaled) transfer time is calculated as 14.9 ps [8.1 ps] with the quantum chemistry set of parameters. The n_1(P+B) → $n_{2,3}$(LH-I) transfer time is calculated as 11.9 ps with the experimental set of parameters.

Conclusions

The rate-limiting step in excitation energy transfer from various light-harvesting complexes to the photosynthetic reaction center has been investigated in this study. The LH-I → RC excitation energy transfer in purple bacterium *Rb. sphaeroides* was studied through Förster theory, based on the crystal structure of the RC and a modeled structure for LH-I. Electronic couplings between LH-I and RC electronic excitations were calculated through the effective Hamiltonian approach presented in [14, 15].

We like to emphasize that the parameters for the effective Hamiltonian which made our analysis possible resulted from a quantum chemical description of the electronic excitations of various BChl aggregates provided in [38]. The latter study was possible only after the pioneering work of Michael Zerner on the semiempirical quantum chemistry program INDO and on the spectra of chlorophylls.

An effective Hamiltonian can easily be constructed with a different set of parameters, and we presented here another effective Hamiltonian based on experimentally determined parameters. The results obtained with the two sets of parameters were compared, and common properties characterizing LH-I → RC excitation energy transfer were observed. These observations are more of a qualitative, than of a quantitative, nature since there are still many uncertainties regarding the nature of electronic excitations, e.g., the delocalization length of LH-I excitons, the nature of RC electronic states.

Another reason arguing against any quantitative predictions lies in the uncertainty of the value of the dielectric constant of the protein medium. The value of the dielectric constant used in our calculations is $\epsilon = 1$. The value often used is $\epsilon = 2.25$. Adjusting the dielectric constant to the value of 2.25 would result in an increase of all transfer times by a factor of 5 (since $\tau \sim 1/k \sim \epsilon^2$).

Both sets of parameters suggest that, within the model of excitons delocalized over the entire LH-I ring, the major pathway of excitation transfer between LH-I and the reaction center involves the strongly optically allowed $n_{2,3}$(LH-I) state. Due to superradiance of the $n_{2,3}$(LH-I) state [and also symmetry characteristics of n_1(P+B)], the n_1(P+B) couplings with this state are stronger than the couplings with Q_y states of individual BChls in LH-I.

The model of completely delocalized excitons is unlikely to be strictly applicable for the LH-I → RC transfer, since most of the experimental estimates suggest that LH-I excitonic coupling in emission at room temperature involves only few BChls. However, superradiance of LH-I emission is still observed, although with a lesser intensity than that of completely delocalized excitons. This would indicate that the coupling of RC states with this emitting state is still stronger than the coupling with individual BChl states, however weaker than that with the $n_{2,3}$(LH-I) state, and we would thus expect that the times of LH-I → RC transfer are inbetween our calculated times of 15.8 ps [$n_{2,3}$(LH-I) → n_1(P+B)] and 102.0 ps [$BChl^M(Q_y)$ → n_1(P+B)].

The back-transfer reaction is found to occur either at the same speed or faster than forward-transfer (depending on the description of LH-I excitons). The spectral overlap for the back-transfer is smaller than the spectral overlap for the forward-transfer, i.e., 4.08 versus 7.26 eV^{-1}. However, in the delocalized exciton picture, the Boltzmann population of the $n_{2,3}$(LH-I) state of only 42.3%, slows down the forward excitation energy transfer, whereas the back-transfer occurs from the almost 100% populated lowest exciton state of the RC. It

is important, however, that back-transfer is slower than the initial electron transfer step in the RC with a reaction time of about 3 ps, which means that the excitation energy trapping by the RC is efficient.

The role of accessory BChls in LH-I → RC excitation transfer was investigated. Accessory BChl excitations most likely mix with the higher exciton state of the special pair. However, poor overlap between the LH-I BChl emission spectrum, and the absorption spectra of all higher exciton states of the RC rule out the possibility that the latter states provide a pathway for LH-I → RC excitation transfer. Only the extremely high couplings between LH-I states and the higher exciton states of the RC could contribute to efficient energy transfer via those states, and these couplings were found to be either of the same order of magnitude or smaller than the couplings with the lowest exciton state. Thus, the lowest exciton state, which consists mainly of the special pair excitations, provides the pathway for excitation transfer and therefore excludes the contribution of the accessory BChls to the excitation transfer.

ACKNOWLEDGMENTS

One of us (K.S.) thanks M. Zerner for a most fruitful collaboration and for his friendship. The authors would like to thank G. Small for important advice and considerable help.

References

1. Hu, X.; Schulten, K. Phys Today 1997, 50, 28.
2. van Grondelle, R.; Dekker, J.; Gillbro, T.; Sundstrom, V. Biochim Biophys Acta 1994, 1187, 1.
3. Fleming, G.; van Grondelle, R. Phys Today 1994, 47, 48.
4. Hu, X.; Damjanović, A.; Ritz, T.; Schulten, K. Proc Natl Acad Sci USA 1998, 95, 5935.
5. van Grondelle, R.; Sundstrom, V. In Sheer, H., Ed.; Photosynthetic Light-Harvesting Systems, Vol. 403; Walter de Gruyter: Berlin, New York, 1988.
6. Visscher, K.; Bergstrom, H.; Sundstrom, V.; Hunter, C.; van Grondelle, R. Photosynth Res 1989, 22, 211.
7. Bergström, H.; van Grondelle, R.; Sundström, V. FEBS Lett 1989, 250, 503.
8. Hess, S.; Chachisvilis, M.; Timpmann, K.; Jones, M.; Fowler, G.; Hunter, C.; Sundstrom, V. Proc Natl Acad Sci USA 1995, 92, 12333.
9. Humphrey, W. F.; Dalke, A.; Schulten, K. J Mol Graphics 1996, 14, 33.
10. Förster, T. Ann Phys (Leipzig) 1948, 2, 55.
11. Hu, X.; Schulten, K. Biophys J 1998, 75, 683.
12. Karrasch, S.; Bullough, P.; Ghosh, R. EMBO J 1995, 14, 631.
13. Jungas, C.; Ranck, J.; Rigaud, J.; Joliot, P.; Vermeglio, A. EMBO J 1999, 18, 534.
14. Hu, X.; Ritz, T.; Damjanović, A.; Schulten, K. J Phys Chem B 1997, 101, 3854.
15. Ritz, T.; Hu, X.; Damjanović, A.; Schulten, K. J Luminescence 1998, 76–77, 310.
16. Leupold, D.; Stiel, H.; Teuchner, K.; Nowak, F.; Sandner, W.; Ucker, B.; Scheer, H. Phys Rev Lett 1996, 77, 4675.
17. Jimenez, R.; Dikshit, S.; Bradforth, S.; Fleming, G. J Phys Chem 1996, 100, 6825.
18. Jimenez, R.; van Mourik, F.; Yu, J. Y.; Fleming, G. R. J Phys Chem B 1997, 101, 7350.
19. Monshouwer, R.; Abrahamsson, M.; van Mourik, F.; van Grondelle, R. J Phys Chem B 1997, 101, 7241.
20. Allen, J.; Yeates, T.; Komiya, H.; Rees, D. Proc Natl Acad Sci USA 1987, 84, 6162.
21. Ermler, U.; Fritzsch, G.; Buchanan, S.; Michel, H. Structure 1994, 2, 925.
22. Feher, G.; Okamura, M. Y. In Clayton, R. K.; Sistrom, W. R., Eds.; The Photosynthetic Bacteria, Vol. 349; Plenum: New York, 1978.
23. Small, G. J. Chem Phys 1995, 197, 239.
24. van Brederode, M. E.; van Grondelle, R. FEBS Lett 1999, 455, 1.
25. Zerner, M. C. In Bicout, D.; Field, M. J., Eds.; Proceedings of the Ecole de Physique des Houches, Vol. 61; Les Editions de Physique, Springer: Paris, 1995.
26. Woodbury, N. W.; Allen, J. P. In Blankenship, R.; Madigan, M.; Bauer, C., Eds.; Anoxygenic Photosynthetic Bacteria, Vol. 527; Kluwer Academic: Dordrecht, 1995.
27. Sim, E.; Makri, N. J Phys Chem B 1997, 101, 5446.
28. Arlt, T.; Bibikova, M.; Penzkofer, H.; Oesterhelt, D.; Zinth, W. J Phys Chem 1996, 12060.
29. Knapp, E. W.; Scherer, P. O. J.; Fischer, S. F. Bioshim Biophys Acta 1986, 852, 295.
30. Won, Y.; Friesner, R. A. J Phys Chem 1988, 92, 2208.
31. Jonas, D. M.; Lang, M. J.; Nagasawa, Y.; Joo, T.; Fleming, G. R. J Phys Chem 1996, 100, 12660.
32. Haran, G.; Wynne, K.; Moser, C. C.; Dutton, P. L.; Hochstrasser, R. M. J Phys Chem 1996, 100, 5562.
33. Somsen, O. J. G.; van Mourik, F.; van Grondelle, R.; Valkunas, L. Biophys J 1994, 66, 1580.
34. Pullerits, T.; Visscher, K. J.; Hess, S.; Sundström, V.; Freiberg, A.; Timpmann, K. Biophys J 1994, 66, 236.
35. Novoderezhkin, V. I.; Razjivin, A. P. Chem Phys 1996, 211, 203.
36. Thompson, M.; Zerner, M. J Am Chem Soc 1991, 113, 8210.
37. Lanthrop, E. J. P.; Friesner, R. A. J Phys Chem 1994, 98, 3056.
38. Cory, M. G.; Zerner, M. C.; Hu, X.; Schulten, K. J Phys Chem B 1998, 102, 7640.
39. Eccles, J.; Honig, B.; Schulten, K. Biophys J 1988, 53, 137.
40. Scherz, A.; Parson, W. W. Biochim Biophys Acta 1984, 766, 653.

41. Koolhaas, M. H. C.; Frese, R. N.; Fowler, G. J. S.; Bibby, T. S.; Georgakopoulou, S.; van der Zwan, G.; Hunter, C. N.; van Grondelle, R. Biochemistry 1998, 37, 4693.
42. Lyle, P. A.; Kolaczkowski, S. V.; Small, G. J. J Phys Chem 1993, 97, 6924.
43. Groot, M.; Yu, J.; Agarwal, R.; Norris, J. R.; Fleming, G. R. J Phys Chem B 1998, 102, 5923.
44. Sebban, P.; Robert, B.; Jolchine, G. Photochem Photobiol 1985, 42, 573.
45. Sauer, K.; Smith, J. R. L.; Schultz, A. J. J Am Chem Soc 1966, 88, 2681.
46. Pearlstein, R. M. Photosynth Res 1992, 31, 213.
47. Visscher, K. J.; Chang, M. C.; van Mourik, F.; Parkes-Loach, P. S.; Heller, B. A.; Loach, P. A.; van Grondelle, R. Biochemistry 1991, 30, 5734.
48. Woodbury, N. W. T.; Parson, W. W. Biochim Biophys Acta 1984, 767, 345.
49. Wu, H.; Small, G. J Phys Chem B 1998, 102, 888.
50. van Oijen, A. M.; Katelaars, M.; Köhler, J.; Aartsma, T. J.; Schmidt, J. Science 1999, 285, 400.
51. Visser, H. M.; Somsen, O. J. G.; van Mourik, F.; van Grondelle, R. J Phys Chem 1996, 100, 18859.